Azetidine-2,4-diones (4-Oxo-β-lactams) as Scaffolds for Designing Elastase Inhibitors

Jalmira Mulchande,[†] Rita C. Guedes,[†] Wing-Yin Tsang,[‡] Michael I. Page,[‡,*] Rui Moreira,[†,*] and Jim Iley[§]

iMed.UL, CECF, Faculdade de Farmácia, Universidade de Lisboa, Av. Forças Armadas, 1600-083 Lisboa, Portugal, Department of Chemical & Biological Sciences, University of Huddersfield, Huddersfield, HD1 3DH, U.K., and Department of Chemistry, The Open University, Milton Keynes, MK7 6AA, U.K.

Received October 5, 2007

A new class of inhibitors 4-oxo-β-lactams (azetidine-2,4-diones), containing the required structural elements for molecular recognition, inhibit porcine pancreatic elastase (PPE) but show a dramatically lower reactivity toward hydroxide compared with the analogous inhibitors 3-oxo-β-sultams. Inhibition is the result of acylation of the active site serine and electron-withdrawing substituents at the *N*-(4-aryl) position in 3,3-diethyl-*N*-aryl derivatives increasing the rate of enzyme acylation and generating a Hammett ρ-value of 0.65. Compared with a ρ-value of 0.96 for the rates of alkaline hydrolysis of the same series, this is indicative of an earlier transition state for the enzyme-catalyzed reaction. Docking studies indicate favorable noncovalent interactions of the inhibitor with the enzyme. Compound **2i**, the most potent inhibitor against PPE, emerged as a very potent HLE inhibitor, with a second-order rate for enzyme inactivation of $\sim 5 \times 10^5$ M^{-1} s^{-1}.

Introduction

Human leukocyte elastase (HLE)[a] is a member of the chymotrypsin superfamily of serine proteases that very efficiently degrades tissue matrix proteins such as elastin when released from the azurophilic granules of polymorphonuclear leukocytes because of inflammatory stimuli and mediators. The imbalance between HLE and its endogenous inhibitors leads to excessive elastin proteolysis and destruction of connective tissues in a number of inflammatory diseases such as pulmonary emphysema, adult respiratory distress syndrome, chronic bronchitis, chronic obstructive pulmonary disease, and rheumatoid arthritis.[1–5]

β-Lactams are well-known as potent inhibitors of some enzymes that contain serine as the catalytic residue, including the bacterial penicillin binding proteins (PBPs) and Class A and Class C β-lactamases.[6] β-Lactams have also been appropriately modified to develop active site-directed and mechanism-based inhibitors of HLE.[7–9] Improvement of the rate of serine acylation by increasing the intrinsic chemical reactivity of the β-lactams has been used as a strategy to design more potent inhibitors.[10] Recently, we have reported that 3-oxo-β-sultam, **1**, is a reasonably potent inhibitor of porcine pancreatic elastase (PPE), a model enzyme that shares ~40% homology and the catalytic triad consisting of Ser-195, His-57 and Asp-102 with HLE. Nucleophilic attack on 3-oxo-β-sultams **1** could involve either acylation or sulfonylation resulting from substitution at the carbonyl center and expulsion of the sulfonamide or from substitution at the sulfonyl center and expulsion of the amide, respectively. Inhibition of elastase by **1** occurs by acylation of the active site serine and so involves C−N fission and expulsion of sulfonamide.[11] By contrast, the alkaline hydrolysis of **1** occurs by hydroxide-ion attack on the sulfonyl center with S−N fission. This is a very rapid process and occurs with a second-order rate constant, k_{OH}, value of $\sim 2 \times 10^5$ M^{-1} s^{-1},[12] which is about 10^6 times higher than those of most clinically useful β-lactams.[13] Highly reactive scaffolds may lead to a decrease the selectivity toward the target enzyme, increase susceptibility to metabolism, and reduce oral bioavailability.[14] The mechanism of inhibition of elastase by **1** involves expulsion of the relatively good leaving sulfonamide group. Selectivity could be improved by replacing this group by a poorer leaving group such as an amide. We now report that isosteric analogues of **1**, azetidine-2,4-diones or 4-oxo-β-lactams, **2**, containing the required structural elements for molecular recognition by PPE and HLE, retain inhibitory activity while dramatically decreasing the reactivity toward hydrolysis by hydroxide ion.

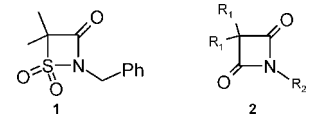

Results and Discussion

Synthesis. 4-Oxo-β-lactams **2** were prepared in reasonable yields from the appropriate 2,2-disubstituted malonic acid chlorides and amines (Scheme 1). The corresponding malondiamides were always obtained as side-products but were easily removed by column chromatography.

Scheme 1

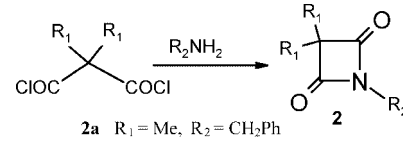

2a R_1 = Me, R_2 = CH_2Ph
2b R_1 = Me, R_2 = C_6H_4-4-Cl
2c R_1 = Et, R_2 = CH_2CO_2Et
2d R_1 = Et, R_2 = CH_2Ph
2e R_1 = Et, R_2 = C_6H_4-4-OMe
2f R_1 = Et, R_2 = C_6H_4-4-Me
2g R_1 = Et, R_2 = C_6H_5
2h R_1 = Et, R_2 = C_6H_4-4-Cl
2i R_1 = Et, R_2 = C_6H_4-4-CN

* To whom correspondence should be addressed. Phone: +44 1484 472531 (M.I.P.). Fax: +44 1484 473075 (M.I.P.). E-mail: m.i.page@hud.ac.uk (M.I.P); rmoreira@ff.ul.pt (R.M.).

† Universidade de Lisboa.

‡ University of Huddersfield.

§ The Open University.

[a] Abbreviations: EREF, enzyme rate enhancement factor; HEPES, *N*-[2-hydroxyethyl]piperazine-*N*′-[2-ethane sulfonic acid]; HLE, Human leukocyte elastase; PBP, penicillin binding proteins; PPE, porcine pancreatic elastase; TI, tetrahedral intermediate.

10.1021/jm701257h CCC: $40.75
Published on Web 02/22/2008

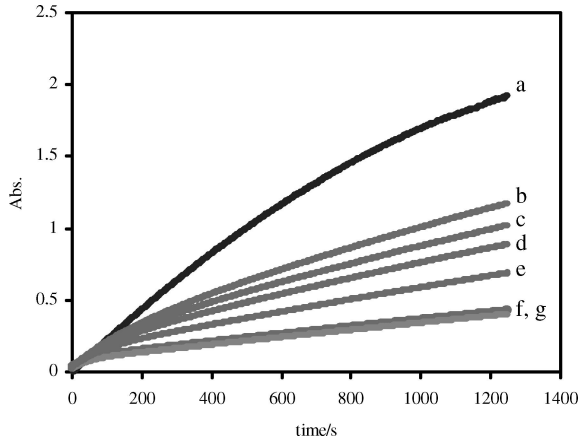

Figure 1. Progress curves for the inhibition of **2h**. Reaction conditions: [PPE] = 0.2 μM, [Suc-(L-Ala)$_3$-*p*-NA] = 0.3 mM, 0.1 M HEPES buffer, pH 7.2, 5% DMSO, 25 °C. Inhibitor concentrations (μM): (a) absence of inhibitor, (b) 10, (c) 15, (d) 20, (e) 30, (f) 60, (g) 75.

Scheme 2

$$E + I \xrightarrow{k_{on}[I]} EI \xrightarrow{k_{deacyl}} E + P$$

PP Elastase Inhibition Studies. Enzyme activity was measured by the hydrolysis of reporter substrate *N*-succinyl-(L-Ala)$_3$-*p*-nitroanilide at 390 nm. Incubation of PPE with 4-oxo-β-lactams **2** resulted, in most cases, in very rapid time-dependent loss of activity (Figure 1), followed by a slower reactivation of enzyme activity. This is presumably attributable to acylation of the active site serine followed by slow hydrolysis and is described by Scheme 2, where EI corresponds to the acyl-enzyme. Therefore, inhibition was studied at 25 °C using the progress curve method,[15] and the time courses for Figure 1 were fit by nonlinear regression analysis to eq 1

$$A = v_s t + (v_i - v_s)(1 - e^{-k_{obs}t})/k_{obs} + A_0 \quad (1)$$

where A is the absorbance at 390 nm, A_0 is the absorbance at $t = 0$, v_i is the initial rate of change of absorbance, v_s is the steady-state rate, and k_{obs} is the first-order rate constant for the approach to the steady-state. The plots of k_{obs} versus the concentration of **2** were linear and thus were consistent with the inhibition mechanism depicted in Scheme 2, which corresponds to eq2.[16] The linear dependence of k_{obs} on [I], as well as the observation that initial velocities, v_i, equalled the velocity in the absence of inhibitor, v_0, suggest that the acyl-enzyme EI did not accumulate in the inhibitor concentration range used. The graphical interpretation (Figure 2) of eq. 2 yields the second-order rate constant for inhibition, k_{on}, as the slope (Table 1) and the first-order rate for deacylation, k_{deacyl}, as the intercept. The K_i values were calculated as k_{deacyl}/k_{on}.

$$k_{obs} = (k_{on}[I]/\{1 + ([S]/K_m)\}) + k_{deacyl} \quad (2)$$

An important criterion for the successful inhibition of serine enzymes by an acylation process depends upon the lifetime of the acyl-enzyme intermediate. A reactive intermediate will undergo rapid hydrolysis as in the normal pathway for the hydrolysis of substrates. In contrast to the slow-binding inhibition model displayed by 3,3-diethyl-substituted 4-oxo-β-lactams, **2e**−**i**, their 3,3-dimethyl counterparts, **2a** and **b** presented strictly linear time courses for the hydrolysis of substrate, that is, no initial exponential phase toward a steady-state was observed. Incubation of 7.5 × 10^{-4} M of *N*-benzyl-4,4-dimethyl-4-oxo-

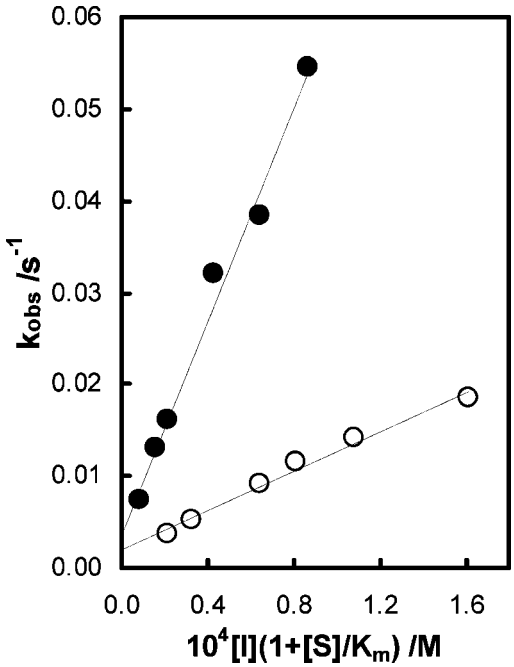

Figure 2. Effect of inhibitor concentration on the onset of inhibition of PPE by **2e** (○) and **2i** (●). Inhibitor concentration is corrected according to eq 2.

β-lactam **2a**, which was in 750-fold excess to PPE concentration, showed no decrease of enzyme activity when the incubated enzyme was diluted into assay cells containing the substrate. The less sterically hindered dimethyl derivative may act as a simple substrate for elastase. However, the reaction of **2a** with elastase was followed by UV-spectroscopy at 242 nm. The plot of absorbance versus time displayed biphasic kinetics, in which the concentration of 4-oxo-β-lactam **2a** decreases with time in a zero-order manner in the first phase of the reaction but changed to first-order kinetics in the second phase of the reaction. This apparent "saturation" behavior is compatible with slow deacylation of the acyl-enzyme intermediate, assuming the exponential decay of absorbance against time for the second phase of the reaction is caused by the hydrolysis of the ring-opened hydrolysis product (Scheme 3). The rate of formation and breakdown of the acyl-enzyme was obtained by fitting the absorbance versus time curve for the reaction of **2a** at high concentration of PPE to Scheme 2 using Dynafit,[17] and the derived rate constants are given in Table 1. Increasing the enzyme concentration did not affect the rate of breakdown of the acyl enzyme intermediate but increased the rate of formation of the acyl-enzyme intermediate. Zero-order kinetics were observed if the rate of acylation is at least 30-fold greater than that of deacylation.

Interestingly, the rate of acylation in the reaction of *N*-benzyl-3,3-dimethyl-4-oxo-β-lactam **2a** with PPE elastase is 12-fold slower than that of inhibition by its 3-oxo-β-sultam counterpart **1** (**1**, k_{on} = 7.68 × 10^2 M^{-1} s^{-1}),[11] with the same enzyme and at pH 6.0, whereas the rate of deacylation in the reaction of **2a** is 500-fold faster than that of the reactivation of the enzyme inhibited with **1** (**1**, k_{deacyl} = 2.08 × 10^{-5} s^{-1}). Nucleophilic attack at the carbonyl center of **1** and that of **2** generates a sulfonamide and an amide leaving group, respectively. Although sulfonamides and amides have different electronic properties, for example, sulfonamides are generally more acidic than amides by about 5 pK_a units,[18] the stability of the acyl ester of the acyl enzymes is unlikely to be affected by this property because the groups are some distance from the acyl ester.[19] However, the

Table 1. Kinetic Parameters for the Inhibition of PPE at pH 7.2 by, and for the Alkaline Hydrolysis of, Azetidin-24-diones, 2, at 25 °C

compound	R^1	R^2	K_i (μM)	k_{on} ($\times 10^{-2}$ M^{-1} s^{-1})	k_{off} ($\times 10^{3}$ s^{-1})	k_{OH^-} (M^{-1} s^{-1})	EREF
2a	Me	CH_2Ph	184	0.63[a]	0.997[a]	1.80[b]; 8.38[c]	
2b	Me	C_6H_4-4-Cl	10.0			9.67	
2c	Et	CH_2CO_2Et	NI	NI		ND	
2d	Et	CH_2Ph	NI	NI		0.0742	
2e	Et	C_6H_4-4-OMe	9.81	1.22	1.20	0.225	542
2f	Et	C_6H_4-4-Me	7.46	1.74	1.30	0.240	725
2g	Et	C_6H_5	10.2	1.77	1.81	0.336	527
2h	Et	C_6H_4-4-Cl	8.47	2.32	1.97	0.581	400
2i	Et	C_6H_4-4-CN	6.02	5.83	3.53	1.78	328

[a] pH 6.0. [b] $T = 30$ °C, 1% DMSO (v/v). [c] $T = 25$ °C, 20% CH_3CN (v/v).

Scheme 3

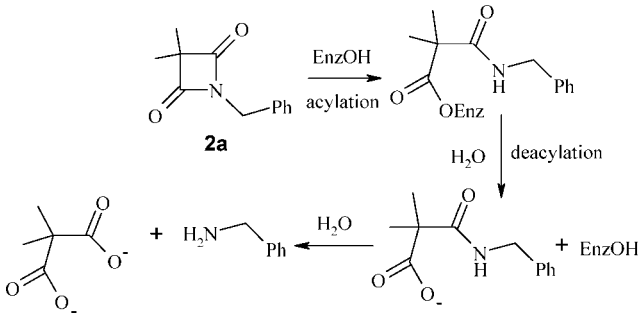

α-tertiary center containing a *gem*-dimethyl group together with a sulfonyl group of a sulfonamide, **3**, is likely to significantly block attack by water at the active site, and the deacylation would be severely impaired. If this is the case, the sulfonamide leaving group being bigger in size, as in **3**, decreases the rate of deacylation by 500-fold compared with that observed with an amide leaving group, **4**.

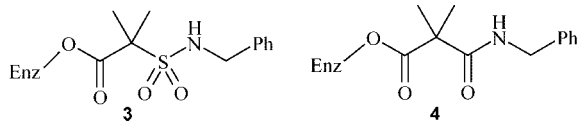

The effect of bulky substituents on the rate of deacylation is also demonstrated by the PPE catalyzed hydrolysis of *N*-benzoyl-3,3-dimethyl-β-lactam **5** (Scheme 4), which shows normal hydrolytic behavior and no accumulation of the acyl enzyme intermediate despite the presence of an α-*gem*-dimethyl group. The acyl enzyme generated from **5** has the structure **6** and presumably moving the exocyclic carbonyl further down the carbon chain in the ring-opened product **6** must reduce the steric congestion around the acyl enzyme ester, allowing rapid deacylation.

Alkaline Hydrolysis. The second-order rate constants, k_{OH}, for the alkaline hydrolysis of the 4-oxo-β-lactams **2** were also determined for comparison with those for PPE inhibition (Table 1). It has been suggested that the magnitude of the second-order rate constant, k_{OH}, for the alkaline hydrolysis of potential inhibitors of enzymes containing a catalytic serine is a crude indicator for their ability to be effective and therapeutically useful acylating agents.[14,20,21] As a result of the symmetry of 4-oxo-β-lactams **2**, the two acyl centers are equivalent, and the hydrolysis products of 4-oxo-β-lactams **2** are the corresponding α-amido acids **7**. The second-order rate constant, k_{OH}, for the alkaline hydrolysis of **2a** is 8.38 M^{-1} s^{-1} (Table 1), which is, remarkably, only 7-fold greater than that for the corresponding *N*-benzoyl-β-lactam **5** and demonstrates the surprisingly small effect of introducing a second sp^2 center into the already strained four-membered ring. Furthermore, the strained cyclic imide **2a** shows reactivity similar to that of the acyclic imide **8** (k_{OH} = 1.54 M^{-1} s^{-1}), [14] showing that there is no significant rate enhancement caused by ring strain, compatible with the limiting step of alkaline hydrolysis being the formation of the tetrahedral intermediate (TI).

Scheme 4

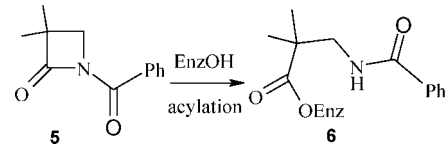

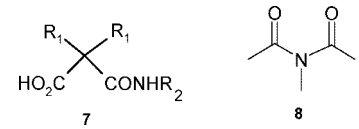

It is of interest to compare the rate constants for alkaline hydrolysis for a series of four-membered rings β-lactams, **2** and **5**, and β-sultams, for example, **1**, with those for their reactions with elastase. The substitution of the *N*-benzyl by *N*-phenyl in 4-oxo-β-lactam changes the leaving group from an amide to an anilide and causes an increase in the rate of ring opening by hydroxide ion (e.g., **2g** is 5-fold more reactive than **2d**). N-Substitution would be expected to have a large effect on rate-limiting C−N fission but a much smaller one if nucleophilic attack on the carbonyl carbon and formation of the tetrahedral intermediate is the rate-limiting step. Electron-withdrawing substituents (such as 4-cyanophenyl **2i** and 4-chlorophenyl **2h**) produce a modest increase in the rate of the alkaline hydrolysis, whereas electron-donating groups (4-methoxyphenyl, **2e**), decrease k_{OH}. Overall, **2i** is nearly 8-fold more active than **2e**. These relative rates indicate that the rate-limiting step is hydroxide-ion attack and formation of the tetrahedral intermediate.

There is a large steric effect of substituents α to the carbonyl carbon on the rate of alkaline hydrolysis. The α-*gem*-diethyl compounds **2d** and **2h** are about 20-fold less reactive than the corresponding α-*gem*-dimethyl compounds **2a** and **2b**, which is also compatible with rate limiting formation of the tetrahedral intermediate.

Structure–Activity Relationships and Molecular Modeling. Inspection of Table 1 indicates that the most potent inhibitors contain an *N*-aryl group in addition to two ethyl groups at C-3. In contrast, *N*-alkyl-4-oxo-β-lactams are either inactive (**2c**, **d**) or weak inhibitors (**2a**) that regenerate the active enzyme. This suggests that the leaving group ability of the amide formed from the decomposition of the tetrahedral intermediate (TI) **9** contributes significantly to the time-dependent inhibition of PPE. The most-active inhibitor contains a 4-CN electron-withdrawing substituent on the *N*-aromatic ring (**2i**) and is nearly 5-fold more potent than **2e**, which contains an electron-donating substituent. Interestingly, log k_{on} values correlate with Hammett σ_p values,

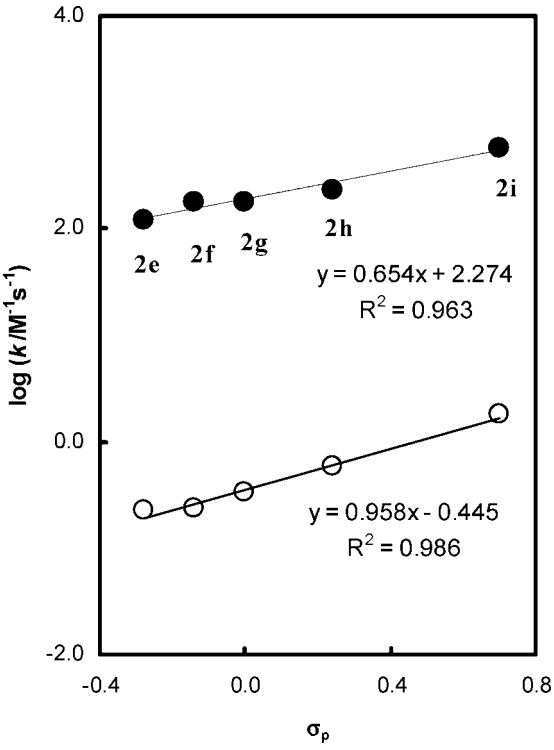

Figure 3. Hammett plots for the second-order rate constants, k_{on}, for the inhibition of PPE by 4-oxo-β-lactams **2e**−**i** (●) and for the hydroxide-ion-catalyzed hydrolysis, k_{OH^-}, of the same compounds (○) at 25 °C.

giving a ρ value of 0.65 (Figure 3), consistent with the reduction of the positive charge on the nitrogen amide caused by resonance rather than the development of significant negative charge on this atom in the transition-state. This is consistent with rate limiting formation of the tetrahedral intermediate in the enzyme catalyzed reaction. In comparison, the alkaline hydrolysis of 4-oxo-β-lactams gives a Hammett ρ value of 0.96 (Figure 3) suggesting a much greater change in charge on going to the transition state. Both enzyme-catalyzed acylation and alkaline hydrolysis of the 4-oxo-β-lactams involve nucleophilic attack on the β-lactam carbonyl. The different Hammett ρ values indicate the enzyme-catalyzed attack of serine occurs at an earlier position along the reaction coordinate leading to formation of the tetrahedral intermediate compared with the hydroxide-ion-catalyzed hydrolysis. This is consistent with the Hammond postulate in that these results suggest that the 4-oxo-β-lactam scaffold promotes the enzyme's ability to use its catalytic apparatus to stabilize the transition state and increase the rate of serine acylation, which might be achieved by favorable noncovalent binding of enzyme and inhibitor, stabilization of the TI in the oxyanion hole of the active site and compensation for the entropy loss required in the bimolecular reaction.

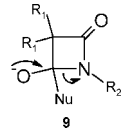

9

It has been suggested that the effectiveness of an enzyme in catalyzing a reaction can be indicated by the enzyme rate enhancement factor, EREF, which is evaluated by dividing the second-order rate constant for the enzyme catalyzed reaction, k_{on}, by that for hydrolysis of the same substrate catalyzed by hydroxide ion, k_{OH}.[14] The highest value of EREF was obtained for inhibitor **2f**: the enzyme increases the rate of reaction by 725-fold.

To rationalize the trends observed in the enzyme assays, the molecular interactions between the more active 4-oxo-β-lactams **2a**, **2e**, **2i** and HLE were investigated using the automated GOLD docking program (see Experimental Section for details). The primary recognition pocket, S_1, for porcine elastase prefers small hydrophobic substituents with two carbon atoms.[22] Docking of the most potent compound, **2i**, into the active site of PPE revealed that only one ethyl substituent of the 3,3-diethyl group lies in the S_1 pocket (Figure 4). This binding mode is not much different than that observed for the interaction of 3,3-diethyl-β-lactams with HLE, in which both ethyl substituents are accommodated in the larger S_1 pocket.[10] The distance between the Ser-195 hydroxyl oxygen atom and the closest carbonyl carbon of **2i** is 3.18 Å (4.79 Å for the other carbonyl carbon atom), which indicates that nucleophilic attack by Ser-195 to the 4-oxo-β-lactam is possible. Interestingly, the "reactive" carbonyl of **2i** is not involved in the H-bond network with the so-called oxyanion hole defined by the backbone NHs of Gly-193 and Ser-195: the distances between the amidic hydrogen atoms of Gly-193 and Ser-195 to the carbonyl oxygen atom are 6.75 and 5.28 Å, respectively. This result may indicate that the oxyanion hole is not used to stabilize the TI derived from **2i**. However, several key interactions seem to stabilize **2i** in the active site. First, strong hydrogen bonds involve the oxygen atom of the reactive carbonyl and the NH of His-57 and the hydroxyl group of Ser-195. Second, an additional hydrogen bond involves the oxygen atom of the unreactive carbonyl and the amide group of Gln-192. Finally, enhanced van der Waals contacts between the N-aryl moiety with Val-99, Phe-215, and His-57 were observed.

For compound **2e**, a less potent inhibitor, an inverted binding mode was observed, in which the 4-OMe substituent of the aromatic ring lies on the S_1 pocket, while one of the ethyl substituents is close to the S_1' pocket (Figure 4). The distance between the closest carbonyl carbon and the Ser-195 hydroxyl oxygen atom is 3.62 Å (4.38 Å for the other carbonyl carbon atom). However, in contrast to **2i**, the reactive carbonyl of **2e** is involved in the H-bond network with the NHs of Gly-193 and Ser-195, which suggests that the oxoanion hole may be used to stabilize the resulting TI and to compensate the energy required for the enzyme to overcome the distance between Ser-195 and the carbonyl carbon. The 3,3-dimethyl-*N*-benzyl derivative **2a** also interacts with PPE with a similar binding mode to that of **2e**, that is, aromatic ring lying on the S_1 pocket (Figure 4) and with the reactive carbonyl involved in the oxoanion hole H-bond network. Compound **2f** also presents the *N*-aryl moiety sitting in the S_1 pocket of the enzyme (see Supporting Information), but in this case, the distance between the closest carbonyl carbon and the Ser-195 hydroxyl oxygen atom is 3.27 Å, that is, close to that of **2i**. This binding confirmation suggests that nucleophilic attack by Ser-195 to the 4-oxo-β-lactam is feasible and is consistent with the EREF value of 725, the highest of the present series of compounds **2**.

Because the 4-oxo-β-lactam inhibitors **2** have two acyl centers, there could be interaction of either the C-3 or the N-1 substituents with the S_1 binding pocket. In principle, the latter could reduce the rate of acylation as a result of nonproductive binding. However, the dominant effect of N-substituents is their influence the rate of C-N bond fission in breakdown of the TI **9**. Compound **2h**, containing a diethyl substituent at C-3 position is a time dependent and, effectively, irreversible inhibitor of

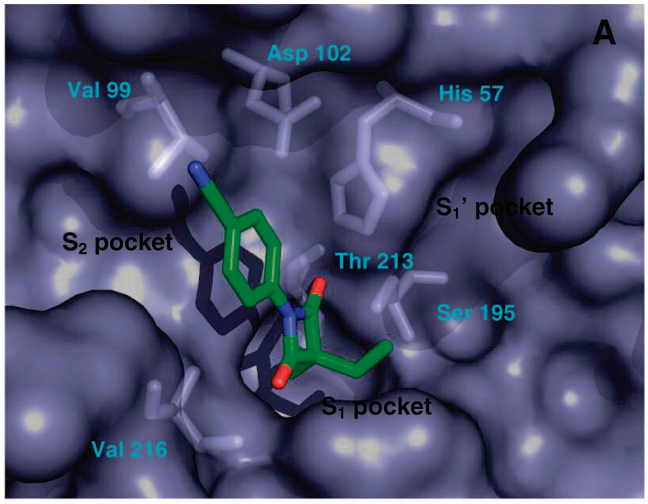

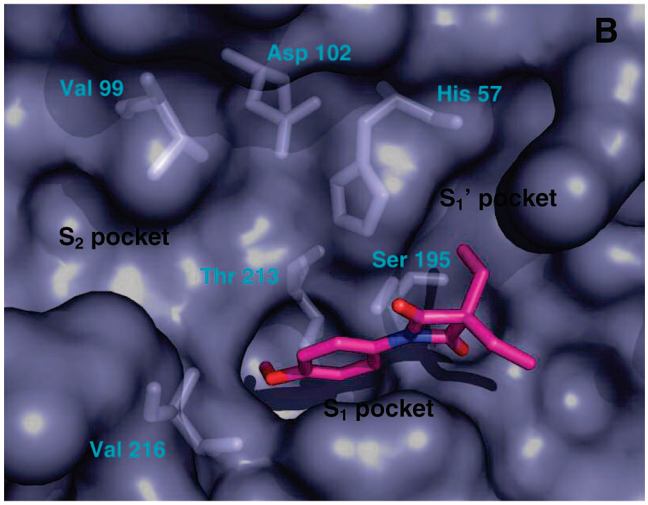

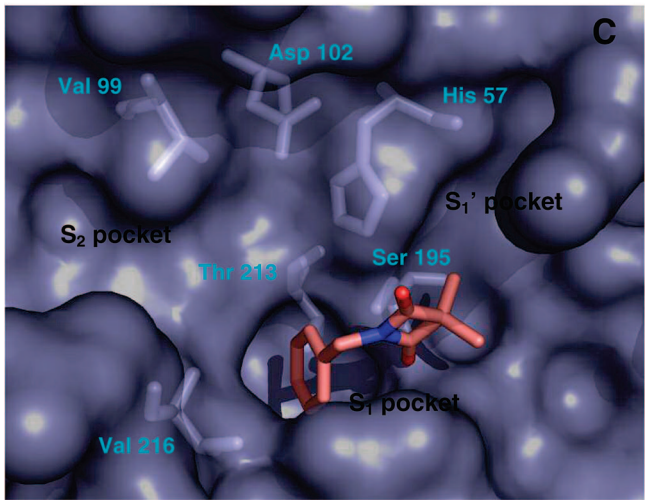

Figure 4. Docking of **2i** (A), **2e** (B), and **2a** (C) in the active site of PPE (see text for details of docking procedure).

PPE because of its relatively fast acylation of the enzyme, while the dimethyl counterpart **2b** is also a time dependent inhibitor, but because of a relatively facile deacylation pathway of the dimethyl acyl-enzyme does allow the enzyme to turnover. The almost complete recovery of enzymatic activity (Figure 5), monitored by checking the enzyme activity at different time intervals after incubation with **2h,** suggests that the interaction of **2** with PPE leads to an labile acyl-enzyme, EI, which breaks

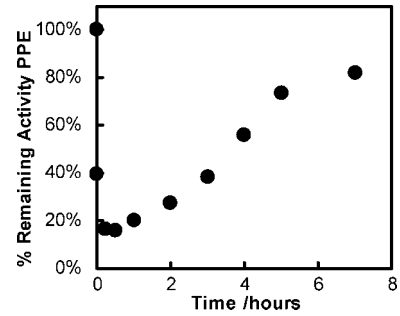

Figure 5. Time-dependent loss of enzymatic activity. Excess of inhibitor **2h** ($[I]_f = 150\ \mu M$) was incubated with PPE ($[E]_f = 10\ \mu M$) in 0.1 M HEPES buffer, pH 7.2, 25 °C, aliquots were withdrawn at different time intervals and assayed for enzymatic activity.

down and regenerates the free, active enzyme, E (Scheme 3), within a few hours and the inhibitor function as alternate substrate inhibitor of PPE.

HLE Inhibition. Taking into account the high k_{on} value obtained for compound **2i** against PPE, we assayed this compound against HLE. A nonlinear dependence of k_{obs} (determined by the progress curve method; eq.1)[15] on inhibitor concentration was observed (Supporting Information) and the individual kinetic parameters K_i (63.5 nM) and k_{inact} (0.0323 s^{-1}) were obtained according to eq 3.[22] The corresponding second-order rate constant for inhibition, k_{inact}/K_i, is 5.08×10^5 $M^{-1}s^{-1}$, a value close to those reported for the most potent monocyclic β-lactams developed by Merck.[22] This result (i) shows the usefulness of the 4-oxo-β-lactam scaffold for designing inhibitors for human elastase and (ii) indicates that **2i** is a promising lead for further optimization against HLE.

$$k_{obs} = k_{inact}[I]/\{K_i(1 + [S]/K_m) + [I]\} \quad (3)$$

Conclusion

This study has shown that 4-oxo-β-lactam derivatives can function as novel time dependent irreversible inhibitors of serine proteases when they contain 3,3-diethyl-*N*-aryl substituents. The title compounds were designed as a result of an isosteric replacement from 3-oxo-β-sultam, yielding more stable compounds to hydrolysis by nonspecific nucleophiles and reacting with the enzyme as active-site-directed inhibitors. The most-active inhibitors correspond to the most reactive compounds toward alkaline hydrolysis and contain electron-withdrawing substituents on the aromatic ring that increase the chemical reactivity of the carbonyl carbon toward nucleophilic attack of the Ser-195 hydroxyl group. The enzyme-mediated hydrolysis has an earlier transition state because of favorable hydrophobic and other noncovalent binding interactions between enzyme and inhibitor that can be used to compensate for unfavorable processes that contribute to the activation energy. In summary, 4-oxo-β-lactam derivatives represent an attractive new class of acyl-enzyme inhibitors of elastases and are suitable scaffolds that might find further applicability for the design of nonpeptidic inhibitors of other serine proteases.

Experimental Section

General. Melting points were determined using a Kofler camera Bock Monoscope M and are uncorrected. The infrared spectra were collected on a Nicolet Impact 400 FTIR infrared spectrophotometer, and the NMR spectra were collected on a Brucker 400 Ultra-Shield (400 MHz) in $CDCl_3$; chemical shifts, δ, are expressed in ppm, and coupling constants, J, are expressed in Hz. Low-resolution mass spectra were recorded using a HP5988A spectrometer, by RIAIDT, University of Santiago de Compostela, Spain. Elemental analyses

were performed by Medac Ltd., Brunel Science Centre, Englefield Green Egham TW20 0JZ, U.K., or by ITN, Chemistry Unit, Sacavém, Portugal. UV spectra and spectrophotometric assays were performed using Shimadzu UV-1603 or UV-2100 PC spectrometers. Thin layer chromatographys were performed on a Merck grade aluminum plates, silica gel 60 F_{254}, and visualized by UV light or iodine. Preparative column chromatography was performed on silica gel 60 from Merck (70–230 mesh ASTM). Dioxane and TEA were purified and dried before use. Sodium hydroxide and hydrochloric acid solutions were prepared from dilution of standardized Tritisol stock solutions. Solvents and buffer materials for enzyme assays were of analytical reagent grade and were purchased from Merck or Sigma. PPE, MeO-Suc-Ala-Ala-Pro-Val-*p*-NA, and *N*-Suc-Ala-Ala-Ala-*p*NA were purchased from Sigma, and HLE was purchased from Calbiochem.

General Procedure for the Synthesis of Azetidine-2,4-dione Derivatives. To a solution of the appropriate malonyl dichloride (0.015 mol) in dry dioxane (15 mL) was added under a nitrogen atmosphere a primary amine (0.015 mol) in the same solvent (15 mL). Subsequently, a solution of triethylamine (0.036 mol) in dry dioxane (15 mL) was added dropwise during 1.5 h, and the resulting mixture refluxed for 6 h, with the reaction progress being monitored by TLC. After the mixture was cooled, triethylamine hydrochloride was filtered off, and the solvent was removed under reduced pressure yielding a solid (malondiamide), recrystallized from dioxane/hexane. The mother liquor was concentrated under reduced pressure, and the residue was purified by chromatography on silica gel, affording the desired product (azetidine-2,4-dione).

1-Benzyl-3,3-dimethylazetidine-2,4-dione, 2a. Compound **2a** was prepared as described above, using dimethylmalonyl dichloride (2.535 g, 0.015 mol), benzylamine as primary amine (1.622 g, 0.015 mol), and triethylamine (3.649 g; 0.036 mol) as catalyst. The resulting reaction mixture was refluxed for 14 h. The product was purified by chromatography on silica gel, using toluene/ethyl acetate as eluant (from 9.8:0.2 to 9.0:1.0), yielding white crystals (0.122 g, 4%): mp 69–71 °C; Anal. ($C_{12}H_{13}NO_2$) C, N. H calcd 6.45; found 5.95; δ ^{1}H NMR 1.38 (6H, *s*), 4.46 (2H, *s*), 7.33–7.39 (5H, *m*); δ ^{13}C NMR 17.44, 42.78, 60.66, 127.99, 128.17, 129.00, 134.77, 175.05.

1-(4-Chlorophenyl)-3,3-dimethylazetidine-2,4-dione, 2b. Compound **2b** was synthesized as described for **2a**, using dimethylmalonyl dichloride (4.225 g, 0.025 mol) and 4-chloroaniline (2.820 g, 0.025 mol), with the reaction mixture being refluxed for 8 h. The product was purified by column chromatography using hexane/ethyl acetate as eluant (8.4: 1.6) to afford **2b** as white crystals (0.351 g, 6%): mp 81–84 °C; Anal. ($C_{11}H_{10}NO_2Cl$) C, H, N; δ ^{1}H NMR 1.51 (6H, *s*), 7.40 (2H, d, $J = 8.8$), 7.82 (2H, d, $J = 8.8$); δ ^{13}C NMR 17.76, 62.03, 120.33, 129.42, 132.12, 132.81, 172.62.

Ethyl 2-(3,3-Diethyl-2,4-dioxoazetidin-1-yl)acetate, 2c. [23] Compound **2c** was prepared as described for **2a** using diethylmalonyl dichloride (4.925 g, 0.025 mol) and ethyl glycinate hydrochloride (3.475 g, 0.025 mol) but with more than 3 equiv of triethylamine (9.107 g, 0.09 mol). The residue was purified by column chromatography on silica gel using mixtures of toluene and ethyl acetate as eluant to yield a colorless oil (0.920 g, 16%): Anal. ($C_{11}H_{17}NO_4$) C, H, N; δ ^{1}H NMR 1.07 (6H, t, $J = 7.6$), 1.30 (3H, t, $J = 7.2$), 1.82, (4H, q, $J = 7.6$), 4,10 (2H, s), 4,25 (2H, q, $J = 7,2$); Lit.[24] 1.03 (3H, t, $J = 7$), 1.30 (3H, t, $J = 7$), 1.77 (4H, q, $J = 7$), 3.98 (2H, s), 4.21 ((2H, q, $J = 7$); δ ^{13}C NMR 9.27, 14.08, 23.62, 39.28, 62.23, 71.30, 165.93, 173.59.

1-Benzyl-3,3-diethylazetidine-2,4-dione, 2d. Compound **2d** was prepared as described for **2a**, using diethylmalonyl dichloride (2.956 g, 0.015 mol), benzylamine (1.622 g, 0.015 mol) as primary amine, and triethylamine (3.649 g, 0.036 mol) as catalyst. The product was purified by chromatography on silica gel using toluene/ethyl acetate as eluant (from 9.8:0.2 to 9.2:0.8) and then recrystallized from hexane to yield the product as white crystals (0.243 g, 9%): mp 46–47 °C; Anal. ($C_{14}H_{17}NO_2$) C, H, N; δ ^{1}H NMR 0.94 (6H, t, $J = 7.6$), 1.75 (4H, q, $J = 7.6$), 4.48 (2H, s), 7.32–7.37 (5H, m); δ ^{13}C NMR 9.18, 23.67, 42.17, 70.98, 128.14, 128.28, 128.88, 135.06, 174.24.

3,3-Diethyl-1-(4-methoxyphenyl)azetidine-2,4-dione, 2e. Compound **2e** was prepared as described for **2a**, using diethylmalonyl dichloride (2.956 g, 0.015 mol) and 4-anisidine (1.605 g, 0.015 mol) as primary amine. Purified by chromatography on silica gel using toluene/ethyl acetate (9.2:0.8), yielding yellow oil (0.412 g, 11%): Anal. ($C_{14}H_{17}NO_3$) C, H, N; δ ^{1}H NMR 1.08 (6H, t, $J = 7.6$), 1.86 (4H, q, $J = 7.6$), 3.84 (3H, s), 6.94 (2H, d, $J = 8.8$), 7.76 (2H, d, $J = 8.8$); δ ^{13}C NMR 9.25, 23.95, 55.51, 71.94, 114.34, 120.89, 172.25.

3,3-Diethyl-1-(4-tolyl)azetidine-2,4-dione, 2f. Compound **2f** was prepared as described for **2a**, using diethylmalonyl dichloride (2.956 g; 0.015 mol) and 4-toluidine (1.605 g; 0.015 mol). The product was purified by chromatography on silica gel using toluene/ethyl acetate (9:1) as eluant, to afford white crystals (0.343 g, 10%): mp 41–44 °C; Anal. ($C_{14}H_{17}NO_2$) C. H calcd 7.41; found 6.59; N calcd 6.06; found 6.56; δ ^{1}H NMR 1.08 (6H, t, $J = 7.6$), 1.87 (4H, q, $J = 7.6$), 2.37 (3H, s), 7.23 (2H, d, $J = 8.4$), 7.73 (2H, d, $J = 8.4$); δ ^{13}C NMR 9.24, 21.18, 23.95, 72.01, 119.19, 129.75, 131.33, 136.69, 172.27.

3,3-Diethyl-1-phenylazetidine-2,4-dione, 2g. Compound **2g** was prepared as described for **2a**, using diethylmalonyl dichloride (2.956 g, 0.015 mol) and aniline (1.397 g, 0.015 mol). It was purified by column chromatography on silica gel using toluene/ethyl acetate (9.0, 1.0) to give a colorless oil (0.474 g, 15%) (Lit.[24] mp. 86–87 °C): Anal. ($C_{13}H_{15}NO_2$) C, H, N; δ ^{1}H NMR 1.09 (6H, t, $J = 7,6$), 1.88 (4H, q, $J = 7.6$), 7.29 (1H, dt, $J = 7.6, 1.2$), 7.73 (2H, dt, $J = 7.6, 1.2$), 7.86 (2H, dd, $J = 7.6, 1.2$); δ ^{13}C NMR 9.25, 23.96, 72.14, 119.23, 126.76, 129.26, 133.85, 172.26.

1-(4-Chlorophenyl)-3,3-diethylazetidine-2,4-dione, 2h. Compound **2h** was prepared as described for **2a**, using diethylmalonyl dichloride (2.956 g; 0.015 mol) and 4-chloroaniline (1.695 g, 0.015 mol). It was purified by column chromatography on silica gel using toluene/ethyl acetate (8.0, 2.0), yielding the product as white crystals (0.544 g, 14%): mp 43–46 °C; Anal. ($C_{13}H_{14}NO_2Cl$) C, H, N; δ ^{1}H NMR 1.08 (6H, t, $J = 7.6$), 1.88 (4H, q, $J = 7.6$), 7.40 (2H, d, $J = 8.8$), 7.83 (2H, d, $J = 8.8$); δ ^{13}C NMR 9.23, 23.93, 72.38, 120.41, 129.42, 132.12, 132.32, 171.96.

4-(3,3-Diethyl-2,4-dioxoazetidin-1-yl)benzonitrile, 2i. Compound **2i** was prepared as described for **2a**, using diethylmalonyl dichloride (2.956 g; 0.015 mol) and 4-cyanoaniline (1.772 g, 0.015 mol). It was purified by column chromatography on silica gel using hexane/ethyl acetate (8.0, 2.0), to yield the product as white crystals (0.687 g, 19%): mp 106–109 °C; Anal. ($C_{14}H_{14}N_2O_2$) C, H, N; δ ^{1}H NMR 1.09 (6H, t, $J = 7.6$), 1.90 (4H, q, $J = 7.6$), 7.74 (2H, d, $J = 8.8$), 8.03 (2H, d, $J = 8.8$); δ ^{13}C NMR 9.21, 23.96, 72.87, 110.10, 118.14, 119.29, 133.49, 137.19, 171.70.

Chemical Kinetics. For all kinetic experiments, temperatures were maintained at 25.0 ± 0.1 °C, and the ionic strength was adjusted to 0.5 M by addition of $NaClO_4$. Sodium hydroxide solutions were prepared by dilution of standardized Titrisol stock solutions and contained 20% (v/v) CH_3CN. Stock solutions of compounds were prepared in CH_3CN. In a typical run, the reaction was initiated by the addition of a 30 μL aliquot of a 10^{-2} M stock solution of substrate to a cuvette containing 3 mL of the alkaline buffer solution. Curves were analyzed as first-order reactions. The pseudo-first-order rate constants, k_{obs}, were obtained by least-squares treatment of $\log(A_t - A_\infty)$ data, where A_t and A_∞ represent the absorbance at time t and at time infinity, respectively. The wavelengths (nm) used were 221 for **2a** and **2d**, 260 for **2b**, **2f**, and **2h**, 247 for **2e**, 255 for **2g**, and 280 nm for **2i**.

Enzymatic Assays. PPE and HLE were assayed spectrophotometrically by monitoring the release of *p*-nitroaniline at 390 and 410 nm, respectively, from the enzyme mediated hydrolysis of the substrates, *N*-Suc-Ala-Ala-Ala-*p*NA and MeO-Suc-Ala-Ala-Pro-Val-*p*-NA at 25 °C to evaluate whether the inhibition is reversible or irreversible. Inactivation rates for time-dependent inhibition were determined continuously, according to the slow tight-biding inhibition model. Alternatively, in cases where no time-dependent inhibition was observed, the inhibitor constants K_i were calculated from Dixon plots.

Enzyme Inactivation by the Progress Curve Method. For the most-active compounds (**2e**−**2i**), PPE inhibition was analyzed by the progress curve method.[15,25] The enzymatic reactions were initiated by addition of 10 μL of PPE (20 μM in HEPES buffer, 0.1 M, pH 7.2) to a cuvette thermostatted at 25 °C, containing 940 μL of HEPES buffer (0.1 M, pH 7.2), 20 μL of DMSO, 20 μL of substrate (15 mM in DMSO), and 10 μL of inhibitor (**2e**−**2i** in DMSO). The absorbance was continuously monitored at 390 nm for 20 min. The final concentrations were [PPE] = 200 nM, [substrate] = 0.3 mM, and [DMSO] = 5% (v/v). Several inhibitor concentrations from 8 to 150 μM were used. Control assays, in which the inhibitor was omitted, ran linearly. The pseudo-first-order rate constants, k_{obs}, for the inhibition of PPE were determined according to the slow tight-binding inhibition model[15] and involved the fitting of product concentration as a function of time to eq 1 by nonlinear regression analysis using the routine ENZFIT (developed at the Faculty of Pharmacy, Lisbon).

Inactivation of HLE was assayed at 25 °C by mixing 10 μL of HLE stock solution (2 μM in 0.05 M acetate buffer, pH 5.5) to a solution containing 10 μL of inhibitor in DMSO (200 μM), 20 μL of substrate MeO-Suc-Ala-Ala-Pro-Val-*p*-NA (50 mM in DMSO), and 960 μL of 0.1 M HEPES buffer, pH 7.2, and the absorbance was continuously monitored at 410 nm for 20 min.

Enzyme Inactivation by the Incubation Method. [26] In a typical experiment, 50 μL of inhibitor **2h** (3 mM in DMSO) was incubated at 25 °C with 750 μL of HEPES buffer (0.1 M; pH 7.2) and 200 μL of PPE solution of 50 μM in HEPES buffer. Aliquots (100 μL) were withdrawn at different time intervals (30 s, 15 min, 30 min, 1 h, 2 h, 3 h, 4 h, 5 h, and 7 h) and transferred to a cuvette thermostatted at 25 °C, containing 895 μL of HEPES buffer (0.1 M; pH 7.2) and 5 μL of substrate (12.5 mM). The absorbance was monitored at 390 nm for 50 s. The amount of enzyme activity was determined by comparison of the activity of a control assay (containing no inhibitor) with the activity of an enzyme solution containing inhibitor at the same time point. The experiment was repeated using inhibitor **2b** (aliquots withdrawn at 30 s, 2 min, 3.5 min, 5 min, 6.5 min, 21 min, and 60 min).

Molecular Modeling. The geometries of compounds **2** were energy minimized using density functional theory.[27] These calculations were performed with the B3LYP[28] hybrid functional and the 6-31+G(d,p) basis set implemented in Gaussian03 software package.[29] After geometry optimizations, partial charges were included using Amber's Antechamber module[30] (included with Chimera software).[31] The PPE structure used was obtained by deletion from the active site of the ligand present in the crystal structure (the β-lactam ring-opened product of a *N*-sulfonylaryl β-lactam covalently linked to Ser-195; PDB accession code 1BTU).[32] Hydrogen atoms were added, and the correct protonation states of histidine residues were assigned according to their surrounding environment. The PPE structure was energy minimized, and charges were added using the Amber united atom force field,[33] implemented in Chimera software.[31] To assess the quality of our docking results, the ligand derived from the *N*-sulfonylaryl β-lactam was docked back into the 1BTU active site showing a very small root-mean-square deviation (rmsd) when compared with 1BTU crystal structure. Molecular docking studies of inhibitors **2** into the active site of PPE enzyme were performed with the flexible GOLD (Genetic Optimisation for Ligand Docking, version 3.0.1)[34] docking program using the goldscore scoring function.[35] Each ligand was initially energy minimized and then subjected to 10 000 docking runs (with a population size of 100; 100,000 genetic algorithm operations; 5 islands). The top 10 solutions (i.e., those with the highest fitness score) were visually analyzed for (i) the hydrophobic and hydrophilic interactions between the ligand and enzyme surfaces and (ii) the distance between the Ser-195 hydroxyl oxygen atom and the carbonyl carbon atoms of each 4-oxo-β-lactam **2**.

Acknowledgment. This work was supported in part by Fundação para a Ciência e Tecnologia (FCT, Portugal) through the project PTDC/QUI/64056/2006. J.M. acknowledges FCT for the PhD grant SFRH/BD/17534/2004.

Supporting Information Available: Analytical data, complete ref 29, plots of k_{obs} versus [I] for **2f**, **2g**, and **2h** in PPE assays, plot of k_{obs} versus [I] for **2i** in the HLE assay, and superimposition of docked structures of **2b**, **2e**, **2f**, and **2i** in PPE active site. This material is available free of charge via the Internet at http://pubs.acs.org.

References

(1) Barnes, P. J. Chronic obstructive pulmonary disease. *New Engl. J. Med.* **2000**, *343*, 269–280.
(2) Cowan, K. N.; Heilbut, A; Humpl, T.; Lam, C.; Ito, S.; Rabinovitsch, M. Complete reversal of pulmonary hypertension in rats by a serine elastase inhibitor. *Nat. Med.* **2005**, *6*, 698–702.
(3) Ohbayashi, H. Current synthetic inhibitors of human neutrophil elastase in 2005. *Expert Opin. Ther. Pat.* **2005**, *15*, 759–771.
(4) Donnelly, L. E.; Rogers, D. F. Therapy for chronic obstructive pulmonary disease in the 21st century. *Drugs* **2003**, *63*, 1973–1998.
(5) Malhotra, S.; Man, S. F. P.; Sin, D. D. Emerging drugs for the treatment of chronic obstructive pulmonary disease. *Expert Opin. Emerging Drugs* **2006**, *11*, 275–291.
(6) Konaklieva, M. I. β-Lactams as inhibitors of serine enzymes. *Curr. Med. Chem* **2002**, *1*, 215–238.
(7) Powers, J. C.; Asgian, J. L.; Ekicu, Ö. D.; James, K. E. Irreversible inhibitors of serine, cysteine, and threonine proteases. *Chem. Rev.* **2002**, *102*, 4639–4750.
(8) Konaklieva, M. I.; Plotkin, B. J. The relationship between inhibitors of eukaryotic and prokaryotic serine proteases. *Mini-Rev. Med. Chem.* **2004**, *4*, 721–739.
(9) Leung, D.; Abbenante, G.; Fairlie, D. P. Protease inhibitors: Current status and future prospects. *J. Med. Chem.* **2000**, *43*, 305–341.
(10) Moreira, R.; Santana, A. B.; Iley, J.; Neres, J.; Douglas, K. T.; Horton, P. N.; Hursthouse, M. B. Design, synthesis and enzymatic evaluation of N1-acyloxyalkyl- and N1-oxazolidin-2,4-dion-5-yl-substituted β-lactams as novel inhibitors of human leukocyte elastase. *J. Med. Chem.* **2005**, *48*, 4861–4870.
(11) Tsang, W. Y.; Ahmed, N.; Hardling, L.; Hemming, K.; Laws, A. P.; Page, M. Acylation versus sulfonylation in the inhibition of elastase by 3-oxo-β-sultams. *J. Am. Chem. Soc.* **2005**, *127*, 8946–8947.
(12) Ahmed, N.; Tsang, W. Y.; Page, M. I. Acyl vs sulfonyl transfer in *N*-acyl β-sultams and 3-oxo-β-sultams. *Org. Lett.* **2004**, *6*, 201–203.
(13) Page, M. I. The mechanisms of reactions of β-lactams antibiotics. *Adv. Phys. Org. Chem.* **1987**, *23*, 165–270.
(14) Sykes, N. O.; Macdonald, S. J. F.; Page, M. I. Acylating agents as enzyme inhibitors and understanding their reactivity for drug design. *J. Med. Chem.* **2002**, *45*, 2850–2856.
(15) Morrison, J.; Walsh, C. The behaviour and significance of slow binding enzyme inhibitors. *Adv. Enzym.* **1988**, *61*, 201–299.
(16) Stein, R. L.; Strimpler, A. M.; Viscarello, B. R.; Wildonger, R. A.; Mauger, R. C.; Traino, D. A. Mechanism for slow-binding inhibition of human leukocyte elastase by valine-derived benzoxazinones. *Biochemistry* **1987**, *26*, 4126–4130.
(17) Kuzmic, P. Program DYNAFIT for the analysis of enzyme kinetic data: Application to HIV proteinase. *Anal. Biochem.* **1996**, *237*, 260–273.
(18) King, J. F. In *The Chemistry of Sulphonic Acids, Esters and their Derivatives*; Patai, S., Rappoport, Z., Eds.; John Wiley: Chichester, U.K., 1991; pp. 249–259..
(19) Page, M. I. β-Sultams—Mechanism of reactions and use as inhibitors of serine proteases. *Acc. Chem. Res.* **2004**, *37*, 297–303.
(20) Indelicato, J. M.; Pasini, C. E. The acylating potential of γ-lactam antibacterials: Base hydrolysis of bicyclic pyrazolidinones. *J. Med. Chem.* **1988**, *31*, 1227–1230.
(21) Krantz, A.; Spencer, R. W.; Tam, T. F.; Liak, T. J.; Copp, L. J.; Thomas, E. M.; Rafferty, S. P. Design and synthesis of 4H-3,1-benzoxazin-4-ones as potent alternate substrate inhibitors of human leukocyte elastase. *J. Med. Chem.* **1990**, *33*, 464–479.
(22) Knight, W.; Green, B.; Chabin, R.; Gale, P.; Maycock, A.; Weston, H.; Kuo, D.; Westler, W.; Dorn, C.; Finke, P.; Hagmann, W.; Hale, J.; Liesch, J.; MacCoss, M.; Navia, M.; Shah, S.; Underwood, D.; Doherty, J. Specificity, stability, and potency of monocyclic β-lactam inhibitors of human leucocyte elastase. *Biochemistry* **1992**, *31*, 8160–8170.
(23) Golik, U. The synthesis of malonimide derivatives as potential penicillin analogs. *J. Heterocycl. Chem.* **1972**, *9*, 21–24.
(24) Dai, S. A.; Juang, T. Y.; Chen, C. P.; Chang, H. Y.; Kuo, W. J.; Su, W. C.; Jeng, R. J. Synthesis of *N*-aryl azetidine-2,4-diones and polymalonamides prepared from selective ring-opening reactions. *J. Appl. Polym. Sci.* **2007**, *103*, 3591–3599.
(25) Hagmann, W. K.; Kissinger, A. L.; Shah, S. K.; Finke, P. E.; Dorn, C. P.; Brause, K. A.; Ashe, B. M.; Weston, H.; Maycock, A. L.;

Knight, W. B.; Dellea, P. S.; Fletcher, D. S.; Hand, K. M.; Osinga, D.; Davies, P.; Doherty, J. B. Orally active β-lactam inhibitors of human-leukocyte elastase.2. Effect of C-4 substitution. *J. Med. Chem.* **1993**, *36*, 771–777.

(26) Kitz, R.; Wilson, I. B. Esters of methanesulfonic acid as irreversible inhibitors of acetylcholinesterase. *J. Biol. Chem.* **1962**, *12*, 2940–2945.

(27) Parr, R. G.; Yang, W. *Density Functional Theory of Atoms and Molecules*; Oxford University Press: Oxford, U. K., 1989.

(28) (a) Becke, A. D. *J. Chem. Phys.* **1993**, *98*, 5648–5652. (b) Lee, C. T.; Yang, W.; Parr, R. G. *Phys. Rev. B* **1988**, *37*, 785–789.

(29) Frisch, M. J. *Gaussian 03*, revision C.02; Gaussian, Inc.: Wallingford, CT, 2004.

(30) Wang, J.; Wang, W.; Kollman, P. A.; Case, D. A. Automatic atom type and bond type perception in molecular mechanical calculations. *J. Mol. Graph. Model.* **2006**, *25*, 247.

(31) For the UCSF Chimera package from the Resource for Biocomputing, Visualization, and Informatics at the University of CA, San Francisco (supported by NIH P41 RR-01081), see: Pettersen, E. F.; Goddard, T. D.; Huang, C. C.; Couch, G. S.; Greenblatt, D. M.; Meng, E. C.; Ferrin, T. E. UCSF Chimera—A visualization system for exploratory research and analysis. *J. Comput. Chem.* **2004**, *25*, 1605–1612.

(32) Wilmouth, R. C.; Westwood, N. J.; Anderson, K.; Brownlee, W.; Claridge, T. D. W.; Clifton, I. J.; Pritchard, G. J.; Aplin, R. T.; Schofield, C. J. Inhibition of elastase by *N*-sulfonylaryl β-lactams: Anatomy of a stable acyl-enzyme complex. *Biochemistry* **1998**, *37*, 17506–17513.

(33) Cornell, W. D.; Cieplak, P.; Bayly, C. I.; Gould, I. R.; Merz, K. M., Jr.; Ferguson, D. M.; Spellmeyer, D. C.; Fox, T.; Caldwell, J. W.; Kollman, P. A. A second generation force field for the simulation of proteins, nucleic acids and organic molecules. *J. Am. Chem. Soc.* **1995**, *117*, 5179–5197.

(34) CCDC Software Ltd., Cambridge, U.K.

(35) Jones, G.; Willett, P.; Glen, R. C.; Leach, A. R.; Taylor, R. Development and validation of a genetic algorithm for flexible docking. *J. Mol. Biol.* **1997**, *267*, 727–748.

JM701257H